

Search for Heavy Neutral and Charged Leptons in e^+e^- Annihilation at $\sqrt{s} = 161$ and $\sqrt{s} = 172$ GeV

The L3 Collaboration

Abstract

A search for unstable neutral and charged heavy leptons as well as for stable charged heavy leptons has been made at center-of-mass energies $\sqrt{s} = 161$ GeV and $\sqrt{s} = 172$ GeV with the L3 detector at LEP. No evidence for their existence was found. We exclude unstable neutral leptons of Dirac (Majorana) type for masses below 78.0 (66.7), 78.0 (66.7) and 72.2 (58.2) GeV, if the heavy neutrino couples to the electron, muon or tau family, respectively. We exclude unstable charged heavy leptons for masses below 81.0 GeV for a wide mass range of the associated neutral heavy lepton. The production of stable charged heavy leptons with a mass less than 84.2 GeV is also excluded. If the unstable charged heavy lepton decays via mixing into a massless neutrino, we exclude masses below 78.7 GeV.

(Submitted to *Physics Letters B*)

Introduction

Electron-positron colliders are well suited for the search for new heavy leptons with masses up to $m_L \leq E_{\text{beam}}$ [1]. Additional heavy neutral and charged leptons are predicted by various models [2]. The predicted production cross sections are large and final state particles can be identified cleanly. Results on this subject obtained at the Z resonance by LEP and SLC experiments can be found in [3], and more recent results obtained at LEP at $\sqrt{s} = 133 - 172$ GeV can be found in [4]. Here we report on a direct search for unstable sequential neutral heavy leptons (heavy neutrinos), L^0 , of the Dirac or Majorana type, and charged heavy leptons, L^\pm . The data used in this analysis were collected with the L3 detector at LEP during 1996 at $\sqrt{s} = 161$ GeV and $\sqrt{s} = 170 - 172$ GeV with integrated luminosities 10.7 pb^{-1} and 10.2 pb^{-1} , respectively. The L3 detector is described elsewhere [5].

Heavy leptons are pair-produced through the s -channel: $e^+e^- \rightarrow \gamma/Z \rightarrow L^+L^-$, $L^0\bar{L}^0$ like $e^+e^- \rightarrow \mu^+\mu^-$. They are assumed to couple to the photon and the Z in the same way as the known leptons. The total cross sections are in the range of 1–4 pb at masses well below the beam energy and fall as the mass of the lepton approaches the beam energy. For neutral heavy leptons the main difference between Dirac and Majorana neutrino types is the dependence of the cross section on velocity $\beta = P_L/\sqrt{P_L^2 + m_L^2}$: $\sigma_{\text{Dirac}} \propto \beta(3 - \beta^2)$ and $\sigma_{\text{Majorana}} \propto \beta^3$. Due to the β^3 term the cross section for Majorana neutrinos falls more rapidly with mass than the cross section for Dirac neutrinos. From LEP results at the Z resonance [3] the mass of a stable neutral heavy lepton, L^0 , must be greater than 40 GeV. Therefore, in this analysis we assume L^0 to be heavier than 40 GeV.

Three different possibilities for the charged heavy lepton decay modes are considered:

- 1) The charged heavy lepton decays via mixing into light neutrinos, $L^\pm \rightarrow \nu_\ell W^{\pm*}$.
- 2) The charged lepton decays through the weak charged current interaction, $L^\pm \rightarrow L^0 W^{\pm*}$, with L^0 being stable.
- 3) If the associated neutral heavy lepton is heavier than its charged partner and there is no or very small mixing into light neutrinos, then the charged heavy lepton would appear as being stable in the detector.

The decay of a neutral heavy lepton is expected to proceed via mixing with a light lepton ($i = e, \mu, \tau$), $L_i^0 \rightarrow \ell_i^\pm W^{\mp*}$. In this search we consider that neutral heavy leptons couple to electron, muon, or tau families and we neglect the possibility of mixing between light leptons. If the decay proceeds via mixing, the decay amplitude contains a mixing parameter U for the transition from the heavy lepton to the light lepton. The mean decay length, D , as a function of $|U|^2$ and mass is given by [6] $D = \beta\gamma c\tau_L \propto \beta|U|^{-2}m_L^\alpha$, where τ_L is the lifetime of the heavy lepton and $\alpha \approx -6$. This implies that the decay can occur far from the interaction point if the particle has a low mass or a very small coupling. To ensure high detection and reconstruction efficiencies, the search is restricted to L^0 's decaying within 1 cm of the interaction point. This limits the sensitivity to the mixing parameter to $|U|^2 > \mathcal{O}(10^{-12})$.

Event Simulation

The generation of heavy lepton production and decay was done with the TIPTOP [7] Monte-Carlo program. It incorporates initial state radiative corrections and the spin effects on the

decay distribution. For the search we considered the mass range of the heavy leptons between 50 and 85 GeV. For the simulation of background from Standard Model processes the following Monte Carlo programs were used: PYTHIA 5.7 [8] ($e^+e^- \rightarrow q\bar{q}(\gamma)$, Ze^+e^- , ZZ , $W^\pm e^\mp \nu$), KORALZ [9] ($e^+e^- \rightarrow \tau^+\tau^-(\gamma)$), KORALW [10] ($e^+e^- \rightarrow W^+W^-$), PHOJET [11] ($e^+e^- \rightarrow e^+e^-q\bar{q}$), DIAG36 [12] ($e^+e^- \rightarrow e^+e^-\tau^+\tau^-$), and EXCALIBUR [13] ($e^+e^- \rightarrow \bar{f}f\bar{f}f$).

The number of events simulated for each background process corresponds to at least 80 times the luminosity of the collected data, except for $e^+e^- \rightarrow e^+e^-q\bar{q}$ where twice the luminosity of the collected data was simulated. The Monte-Carlo events have been simulated in the L3 detector using the GEANT3 program [14], which takes into account the effects of energy loss, multiple scattering and showering in the materials. The selection efficiency is determined by the Monte Carlo. To obtain mass limits, the selection efficiency has been reduced by one standard deviation of the total systematic error.

Lepton and Jet Identification, and Background Rejection

An electron is identified as a cluster in the electromagnetic calorimeter with an energy larger than 4 GeV matched to a track in the (R, ϕ) plane to within 20 mrad. The cluster profile should be consistent with the one expected for an electron, *i.e.* we require $0.95 < E_9/E_{25} < 1.05$, where $E_{9(25)}$ is the corrected sum of energies of 9(25) BGO crystals around the most energetic one (including the energy of the most energetic one). The electron candidate must have $|\cos\theta| < 0.94$. Muons are measured by the muon chamber system surrounding the calorimeters. We require that a muon track consists of track segments in at least two layers of muon chambers, and that the muon track points back to the interaction region. The muon momentum must be greater than 4 GeV and it must be in the fiducial volume defined by $|\cos\theta| < 0.92$. In the following analysis lepton isolation is also required. The lepton is isolated if the energy in a 30° cone around it, is smaller than 5 GeV. Moreover, for isolated electrons we require only one matched track to eliminate converted photons. Jets are reconstructed from electromagnetic and hadronic calorimeter clusters using the Durham algorithm [15] with a jet resolution parameter of $y_{cut} = 0.008$. The jet momenta are defined by the vectorial energy sum of calorimetric clusters.

The most important backgrounds for the new heavy lepton searches are W^+W^- and $q\bar{q}(\gamma)$ production for the signatures with large visible energy and two-photon processes for the signatures with small visible energy. The two-photon and $q\bar{q}(\gamma)$ processes can be rejected demanding transverse momentum imbalance, the absence of energy in the very forward-backward regions, and a missing momentum vector not pointing to the very forward-backward regions. The cut on the number of hadronic jets in the event is also important. For W^+W^- process rejection, a variety of cuts on visible mass, number of hadronic jets, jet angles and energies, lepton energies, invariant mass of the lepton and unseen neutrino could be used.

Search for Unstable Neutral Heavy Leptons

The event topology used in the search for pair produced heavy neutrinos is two isolated leptons (e , μ , or τ) plus the decay products of real or virtual W bosons, $e^+e^- \rightarrow L^0\bar{L}^0$, $L^0 \rightarrow \ell^\pm W^{\mp*}$. Two sets of cuts are used to search for the final states with two electrons(muons) and taus. For both selections, the visible energy is required to be greater than 60 GeV and the charged track multiplicity to be greater than 3 in order to reject the two-photon background.

For the electron(muon) decay mode, $L^0 \rightarrow e^\pm(\mu^\pm)W^{\mp*}$, events satisfying the following criteria are selected :

- The number of reconstructed jets plus isolated leptons is at least 3;
- The event contains at least two electrons or two muons. At least one lepton in the event is isolated. In addition for the electron decay mode, the energy in a 10° cone around each electron is less than 5 GeV.

After applying the selection, no events are left in the data for the electron and muon decay modes while we expect 0.4 and 0.7 background events, respectively.

For the tau decay mode, $L^0 \rightarrow \tau^\pm W^{\mp*}$, the same selection criteria as for the electron(muon) decay mode is applied to cover the final state when both taus decay into leptons (two electrons, two muons, and electron plus muon in the final state). To cover the final state when a tau decays hadronically into one prong, events satisfying the following criteria were selected :

- The number of reconstructed jets plus isolated leptons is at least 4;
- The polar angle θ of the missing momentum should be in the range $25^\circ < \theta < 155^\circ$, and the fraction of visible energy in the forward-backward region ($\theta < 20^\circ$ and $\theta > 160^\circ$) should be less than 40%;
- The angle between the most isolated track and the track nearest to it, α_1 , should be greater than 40° or the angle between the second most isolated track and the track nearest to it, α_2 , should be greater than 20° . The distributions of $\cos \alpha_1$ versus $\cos \alpha_2$ are shown for data in Figure 1a, and for background and signal Monte Carlo in Figure 1b, after the previous cuts have been applied. The transverse momenta, p_t , of the two most isolated tracks should be greater than 1.0 GeV, and at least one track should have p_t greater than 2.5 GeV.

At $\sqrt{s} = 172$ GeV, the W^+W^- background is much more severe than at $\sqrt{s} = 161$ GeV, due to the much larger production cross section. To reduce this additional background at $\sqrt{s} = 172$ GeV electron and muon energies should be less than 35 GeV. After applying the above selection, 1 event is left in the data, while we expect 2.0 from backgrounds.

The selection efficiency for the 55–80 GeV neutral heavy lepton mass range is 50% for the electron and muon decay modes. For the tau decay mode, the selection efficiency is 35% at $\sqrt{s} = 161$ GeV and 33.5% at $\sqrt{s} = 172$ GeV. The systematic error, which is mainly due to the uncertainties in the energy calibration factors and the lepton identification, is estimated to be 5% relative. Figure 2 shows the expected number of events (combined at $\sqrt{s} = 161$ and $\sqrt{s} = 172$ GeV) and the 95% C.L. lower limit for the cases where the neutral heavy lepton decays into electrons and muons (Figure 2a), or taus (Figure 2b). We exclude the production of unstable Dirac neutrinos at 95% C.L. for masses below 78.0, 78.0 and 72.2 GeV and unstable Majorana neutrinos below 66.7, 66.7 and 58.2 GeV if the additional heavy neutrino couples to the electron, muon and tau family, respectively.

Search for Unstable Charged Heavy Leptons

Decay into light Neutrino, $L^\pm \rightarrow \nu_\ell W^{\pm*}$

For this search, two sets of cuts are used to search for the topology with one hadronic and one leptonic W-decay as well as two hadronic W-decays. For both selections we require, the visible

energy to be greater than 40 GeV, the multiplicity of charged tracks to be greater than 3, the number of jets and isolated leptons to be at least 3, and the fraction of the total visible energy in the forward-backward region ($\theta < 20^\circ$ and $\theta > 160^\circ$) to be less than 25%.

For the mode, $L^+L^- \rightarrow \nu_\ell\nu_\ell W^{+*}W^{-*} \rightarrow \nu_\ell\nu_\ell\ell\nu_\ell q\bar{q}'$, events satisfying the following criteria are selected:

- The event contains at least one isolated electron or muon with energy greater than 4 GeV;
- The polar angle θ of the missing momentum should be in the range $25^\circ < \theta < 155^\circ$;
- The invariant mass of the lepton and missing momentum should be outside the W mass range (less than 65 GeV or greater than 95 GeV), or the angle between the lepton and missing momentum should be less than 140° . Figure 3 shows the distribution of the invariant mass of the lepton and missing momentum, after the previous cuts have been applied. The sum of the energies of the two most energetic hadronic jets should be less than 75 GeV.

After applying the selection, 1(1) events are left in the 161(172) GeV data while we expect 0.5(1.5) from the background Monte Carlo.

For the hadronic mode (both W bosons decay hadronically), events satisfying the following criteria are selected:

- The event should not contain isolated electrons or muons, and the visible mass should be less than 130 GeV;
- The polar angle θ of the missing momentum should be in the range $35^\circ < \theta < 145^\circ$, and the ratio of transverse jet momenta imbalance divided by total visible energy must be greater than 0.15. Figure 4 shows the distribution of the ratio of the transverse momentum imbalance to the total visible energy, after the previous cuts have been applied.
- The maximum angle between any pair of hadronic jets should be less than 150° , and the sum of the energies of the two most energetic hadronic jets should be less than 60 GeV;
- The thrust of the event should be less than 0.85.

After applying the selection, 3(5) events are left in the 161(172) GeV data while we expect 4.3(4.8) from the background Monte Carlo.

The kinematic distributions of the candidates (combining both topologies) are consistent with that expected from background. The selection efficiency for the 60–80 GeV charged heavy lepton mass range is 36.5% at $\sqrt{s} = 161$ GeV and 33.4% at $\sqrt{s} = 172$ GeV. The systematic error, which is mainly due to the uncertainties in the Monte Carlo statistics, the energy calibration factors and the lepton identification, is estimated to be 5% relative. Figure 5a shows the expected number of events (combined at $\sqrt{s} = 161$ and 172 GeV) and the 95% C.L. lower limit. We exclude production of unstable charged heavy leptons at 95% C.L. for masses below 78.7 GeV.

Decay into Heavy Stable Neutrino, $L^\pm \rightarrow L^0 W^{\pm*}$

In our search for a charged heavy lepton, decaying into heavy stable neutrino, we assume that the mass of the associated heavy neutrino L^0 is greater than 40 GeV, which results in a large missing energy and a large transverse momentum imbalance. In the limit of a vanishing mass difference between charged lepton and associated neutral lepton ($\Delta m = m_{L^\pm} - m_{L^0}$), the signal efficiency is limited by the trigger efficiency and the two-photon background. Here the search is restricted to $10 \text{ GeV} \leq \Delta m \leq 35 \text{ GeV}$. The case of a light neutrino ($\Delta m = m_{L^\pm}$) has been considered in the previous section. The main background is the two-photon process for small mass difference ($\Delta m \leq 20 \text{ GeV}$) and the $q\bar{q}(\gamma)$ process for high mass difference ($\Delta m \geq 20 \text{ GeV}$). As in the search for unstable charged lepton decaying into light neutrino, we search for the topology with one hadronic and one leptonic W-decay as well as two hadronic W-decays. For both selections, to reject the two-photon background, the multiplicity of charged tracks is required to be greater than 2, the number of jets and isolated leptons to be at least 3, and the fraction of the total visible energy in the forward-backward region ($\theta < 20^\circ$ and $\theta > 160^\circ$) to be less than 20%.

For the mode, $L^+L^- \rightarrow L^0L^0W^{+*}W^{-*} \rightarrow L^0L^0\ell\nu_\ell q\bar{q}'$, events satisfying the following criteria are selected:

- The event contains at least one isolated electron(muon) with energy greater than 2(3) GeV (In order to maintain high efficiency for small mass difference, Δm , we reduce the minimum energy requirement for identified electrons(muons) described previously);
- The total visible energy is greater than 6 GeV and less than 70 GeV, and the polar angle θ of the missing momentum is in the range $25^\circ < \theta < 155^\circ$;
- The missing momentum is greater than 3.5 GeV, and the transverse momentum imbalance is greater than 2.5 GeV.

After applying the selection, 2 events are left in the data at $\sqrt{s} = 172 \text{ GeV}$ while 2.5 events are expected from background.

For the hadronic mode (both W bosons decay hadronically), events satisfying the following criteria are selected:

- The event does not contain isolated electrons or muons, and the total visible energy is greater than 9 GeV and less than 80 GeV;
- The polar angle θ of the missing momentum is in the range $35^\circ < \theta < 145^\circ$, and the polar angle of the thrust axis is greater than 25° ;
- The transverse momentum imbalance is greater than 6.5 GeV, and the ratio of the transverse jet momenta imbalance divided by the total visible energy is greater than 0.15.

After applying the selection, 5 events are left in the data at $\sqrt{s} = 172 \text{ GeV}$ while 7.2 events are expected from background.

The kinematic distributions of the candidates (combining both topologies) are consistent with that from two-photon processes. The combined trigger and selection efficiency varies from 33% at $\Delta m = 10 \text{ GeV}$ to 64% at $\Delta m = 35 \text{ GeV}$. The estimated systematic error, which is mainly due to the uncertainties in the energy calibration factors and the lepton identification, varies from 5% relative for 30 GeV mass difference up to 7% relative for 10 GeV mass difference. Figure 5b shows the 95% C.L. exclusion contour in the $m_{L^\pm} - m_{L^0}$ mass plane at $\sqrt{s} = 172 \text{ GeV}$. Also shown is the exclusion contour from the previous L3 result at $\sqrt{s} = 133 \text{ GeV}$.

Search for Stable Charged Heavy Leptons

Pair production of new stable charged heavy leptons would appear as two back to back charged tracks in the L3 detector. The momentum of these particles would in general be large, and the tracks would be highly ionising. The dE/dx information from the tracking chamber has been used to search for pair production of stable heavy charged particles. The track energy loss (dE/dx) is defined by a quantity which is corrected for track length and normalized to 1.0 for a $\beta \approx 1$ particle. The dE/dx was calibrated with Bhabha scattering events.

The search was performed using data collected at $\sqrt{s} = 133$ GeV, $\sqrt{s} = 161$ GeV and $\sqrt{s} = 172$ GeV. Events are selected which satisfy the following criteria:

- The events have two reconstructed tracks with distance of closest approach to the beam axis less than 2 mm. The tracks are required to be in the polar angle range defined by $|\cos\theta| < 0.82$.
- Both tracks are required to have momentum greater than 5 GeV and the acollinearity angle between the tracks is less than 15° ;
- The track ionisation energy loss for both tracks is between 1.25 and 8 units.

The first criteria selects events with two well measured tracks in polar angle range for which the trigger and track reconstruction efficiency is high. From independently triggered $e^+e^- \rightarrow e^+e^-$ events, the tracking chamber trigger efficiency was determined to be greater than 95% over the interval $|\cos\theta| < 0.82$. The momentum and acollinearity cuts reduce the background from two photon produced lepton pairs as well as from dilepton annihilation events with a high energy photon in the final state. Most of the events remaining after the momentum and acollinearity cuts have been applied are $e^+e^- \rightarrow e^+e^-$ and $e^+e^- \rightarrow \mu^+\mu^-$ events.

Figure 6 shows, for events in the 172 GeV data passing the above cuts, except that on track ionisation, the scatter of the normalized track ionisation energy loss, dE/dx , for track 2 vs track 1. For stable charged heavy leptons, both tracks should be highly ionising, $dE/dX_{1,2} > 1.25$. No events are observed in the region defined by this cut in any of the three data samples. In figure 6 is also shown the expected signal from pair-production of mass 84 GeV stable heavy charged leptons from a Monte Carlo simulation. For the dE/dx simulation, a fit to the track ionization as a function of β was performed using electrons, pions, muons, and protons of various momenta in the data. The parameterization of the dE/dx was then used to simulate track ionization for the stable charged heavy lepton tracks.

The production of heavy stable leptons has been excluded previously up to $m_{L^\pm} \approx 45$ GeV using LEP1 data [3]. Therefore, in order to estimate background contamination in the signal region, a control sample of 30 pb^{-1} of Z data is used. The average value for dE/dx for events in both the Z data and high energy samples passing the above cuts is 1.0 with a $\sigma_{dE/dx} = 0.08$. The fraction of events in which both tracks have $dE/dx > 1.25$ in the Z data sample is found to be 4×10^{-5} . Assuming that these highly ionising tracks are the result of fluctuations, this leads to an estimate of 0.07 ± 0.05 background events in the combined 130-172 GeV data samples passing all cuts.

For the 172 GeV data, the selection efficiency for passing all the requirements varied from 64% at lepton mass of $m_{L^\pm} = 70$ GeV to 68% at $m_{L^\pm} = 83$ GeV. For $m_{L^\pm} < 68$ GeV and $m_{L^\pm} > 83$ GeV, the efficiency for both tracks to be in the search region drops to zero. The selection efficiency exhibits the same characteristics for the 161 GeV and 130-140 GeV data with approximately constant efficiency of $\sim 65\%$ for masses $0.8E_{\text{beam}}$ to $0.97E_{\text{beam}}$ and

falling outside that range. For $M_L < 0.80 E_{\text{beam}}$, the stable charged heavy lepton would have sufficient kinetic energy to penetrate the calorimeters and make a high momentum track in the muon chambers. The stable charged leptons would then show up as an excess in dimuon event production, mostly at high effective center-of-mass energy $\sqrt{s'} \approx \sqrt{s}$. In the 172 GeV data sample, 32 dimuon event candidates are observed [16] with $\sqrt{s'} > 0.85\sqrt{s}$. The expected number of such events from the Standard Model is 34. For $M_L = 68$ GeV, 12.9 events are expected from the process $e^+e^- \rightarrow L^+L^-$ where L^\pm is dimuon-like in L3. Therefore, from the absence of an excess in dimuon events in the data, we can exclude at 95% C.L., pair-production of stable charged heavy leptons with mass less than 68.2 GeV.

Figure 7 shows the expected number of events (combined for $\sqrt{s} = 130\text{-}172$ GeV) and the 95% C.L. lower limit as a function of mass. The systematic error, estimated to be 8% relative, is mainly due to the uncertainty in the trigger efficiency, the simulation and reconstruction of the heavy leptons, and the Monte Carlo statistics. There were no signal events observed in the data. This corresponds to a mass limit of $m_{L^\pm} > 84.2$ GeV at 95% C.L. Assuming the above efficiency, the absence of a signal for heavy stable charged particles in the data corresponds to an upper limit on the cross section for pair-production of heavy stable charged particles of mass 60-84 GeV and charge $\pm 1e$ of between 0.3-0.5pb at 95% C.L.

Acknowledgements

We wish to express our gratitude to the CERN accelerator divisions for the excellent performance of the LEP machine. We acknowledge with appreciation the effort of all engineers, technicians and support staff who have participated in the construction and maintenance of this experiment.

References

- [1] A. Zichichi *et al.*, Preprint INFN/AE-67/3; Lett. Nuovo Cimento **4** (1970) 1156; Nuovo Cimento **17 A** (1973) 383;
M. Perl *et al.*, Phys. Rev. Lett. **35** (1975) 1489.
- [2] J.D. Bjorken and C.H. Llewellyn Smith, Phys. Rev. **D 7** (1973) 887;
M. Perl and P. Rapidis, Preprint SLAC-PUB-1496 (1974);
J.C. Pati and A. Salam, Phys. Rev. **D 10** (1974) 275; Phys. Lett. **B 58** (1975) 333;
R.N. Mohapatra and J.C. Pati, Phys. Rev. **D 11** (1975) 366,2588;
R.N. Mohapatra and G. Senjanovic, Phys. Rev. **D 12** (1975) 1502; Phys. Rev. Lett. **44** (1980) 912;
J. Maalampi and K. Enqvist, Phys. Lett. **B 97** (1980) 315;
M. Perl, Preprint SLAC-PUB-2752 (1981);
R.E. Shrock, Phys. Rev. **D 24** (1981) 1275;
M. Gronau, C.N. Leung and J.L. Rosner, Phys. Rev. **D29** (1984) 2539;
F.J. Gilman, Comm. Nucl. Part. Phys. **16** (1986) 231;
J. Bagger *et al.*, Nucl. Phys. **B 258** (1985) 565;
J. Hewett and T.G. Rizzo, Phys. Rep. **183** (1989) 193;
J. Maalampi and M. Roos, Phys. Rep. **186** (1990) 53;
C.T. Hill and E.A. Paschos, Phys. Lett. **B 241** (1990) 96;
W. Buchmüller and C. Greub, Nucl. Phys. **B 363** (1991) 345; Nucl. Phys. **B 381** (1992) 109;
A. Datta and A. Pilaftsis, Phys. Lett. **B 278** (1992) 162;
A. Djouadi, Z. Phys. **C 63** (1994) 317.
- [3] ALEPH Collaboration, D. Decamp *et al.*, Phys. Lett. **B 236** (1990) 511;
ALEPH Collaboration, D. Decamp *et al.*, Phys. Rep. **216** (1992) 253;
DELPHI Collaboration, P. Abreu *et al.*, Nucl. Phys. **B 367** (1991) 511;
DELPHI Collaboration, P. Abreu *et al.*, Phys. Lett. **B 274** (1992) 230;
L3 Collaboration, B. Adeva *et al.*, Phys. Lett. **B 251** (1990) 321;
L3 Collaboration, O. Adriani *et al.*, Phys. Rep. **236** (1993) 1;
OPAL Collaboration, M.Z. Akrawy *et al.*, Phys. Lett. **B 240** (1990) 250;
OPAL Collaboration, M.Z. Akrawy *et al.*, Phys. Lett. **B 247** (1990) 448;
OPAL Collaboration, M.Z. Akrawy *et al.*, Phys. Lett. **B 252** (1990) 290;
OPAL Collaboration, G. Alexander *et al.*, Z. Phys. **C 52** (1991) 200;
MARK II Collaboration, G.S. Abrams *et al.*, Phys. Rev. Lett. **63** (1989) 2447;
MARK II Collaboration, G.K. Jung *et al.*, Phys. Rev. Lett. **64** (1990) 1091;
MARK II Collaboration, P.R. Burchat *et al.*, Phys. Rev. **D 41** (1990) 3542;
MARK II Collaboration, E. Soderstrom *et al.*, Phys. Rev. Lett. **64** (1990) 2980.
- [4] ALEPH Collaboration, D. Buskulic *et al.*, Phys. Lett. **B 384** (1996) 439;
ALEPH Collaboration, R. Barate *et al.*, Preprint CERN-PPE/97-041 to be published in Phys. Lett. **B**;
DELPHI Collaboration, P. Abreu *et al.*, Phys. Lett. **B 396** (1997) 315;
L3 Collaboration, M. Acciarri *et al.*, Phys. Lett. **B 377** (1996) 304;
OPAL Collaboration, G. Alexander *et al.*, Phys. Lett. **B 385** (1996) 433;
OPAL Collaboration, K. Ackerstaff *et al.*, Phys. Lett. **B 393** (1997) 217.

- [5] L3 Collaboration, B. Adeva *et al.*, Nucl. Instr. Meth. **A 289** (1990) 35;
M. Acciari *et al.*, Nucl. Instr. Meth. **A 351** (1994) 300;
M. Chemarin *et al.*, Nucl. Instr. Meth. **A 349** (1994) 345;
M. Adam *et al.*, Nucl. Instr. Meth. **A 383** (1996) 342;
G. Basti *et al.*, Nucl. Instr. Meth. **A 374** (1996) 293.
- [6] M. Gronau, C. Leung and J. Rosner, Phys. Rev. **D29** (1984) 2539.
- [7] S. Jadach and J. Kühn, TIPTOP Monte Carlo, Preprint MPI-PAE/PTh 64/86.
- [8] PYTHIA Monte Carlo Program: T. Sjöstrand, Comp. Phys. Comm. **82** (1994) 74.
- [9] S. Jadach, J. Kühn and Z. Was, Comp. Phys. Comm. **64** (1991) 275;
S. Jadach, B.F.L.Ward and Z. Was, Comp. Phys. Comm. **66** (1991) 367.
- [10] Monte Carlo program KORALW 1.02.
M. Skrzypek, S.Jadach, W. Placzek and Z. Was, CERN preprint CERN-TH/95-205, to be published in Comp. Phys. Comm.
- [11] R. Engel, Z. Phys. **C 66** (1993) 1657.
- [12] F.A. Berends, P.H. Daverveldt and R. Kleiss, Nucl. Phys. **B 253** (1985) 421; Comp. Phys. Comm. **40** (1986) 271.
- [13] F.A. Berends, R. Kleiss and R. Pittau, Nucl. Phys. **B424** (1994) 308; Nucl. Phys. **B426** (1994) 344; Nucl. Phys. (Proc. Suppl.) **B37** (1994) 163; Phys. Lett. **B 335** (1994) 490;
R. Kleiss and R. Pittau, Comp. Phys. Comm. **83** (1994) 141.
- [14] The L3 detector simulation is based on GEANT Version 3.15. See R. Brun et al., "GEANT 3", CERN DD/EE/84-1 (Revised), September 1987. The GHEISHA program (H. Fesefeldt, RWTH Aachen Report PITHA 85/02 (1985)) is used to simulate hadronic interactions.
- [15] Y.L. Dokshitzer, Contribution to the Workshop on Jets at LEP and HERA, Durham (1990);
N. Brown and W.J. Stirling, Rutherford Preprint RAL-91-049;
S. Catani *et al.*, Phys. Lett. **B 269** (1991) 432;
S. Bethke *et al.*, Nucl. Phys. **B 370** (1992) 310.
- [16] L3 Collaboration, M. Acciarri *et al.*, Preprint CERN-PPE/97-052 to be published in Phys. Lett. **B**.

The L3 Collaboration:

M. Acciarri,²⁹ O. Adriani,¹⁸ M. Aguilar-Benitez,²⁸ S. Ahlen,¹² J. Alcaraz,²⁸ G. Alemani,²⁴ J. Allaby,¹⁹ A. Aloisio,³¹ G. Alverson,¹³ M.G. Alviggi,³¹ G. Ambrosi,²¹ H. Anderhub,⁵¹ V.P. Andreev,^{7,40} T. Angelescu,¹⁴ F. Anselmo,¹⁰ A. Arefiev,³⁰ T. Azemoon,³ T. Aziz,¹¹ P. Bagnaia,³⁹ L. Baksay,⁴⁶ S. Banerjee,¹¹ Sw. Banerjee,¹¹ K. Banicz,⁴⁸ A. Barczyk,^{51,49} R. Barillère,¹⁹ L. Barone,³⁹ P. Bartalini,³⁶ A. Baschirotto,²⁹ M. Basile,¹⁰ R. Battiston,³⁶ A. Bay,²⁴ F. Becattini,¹⁸ U. Becker,¹⁷ F. Behner,⁵¹ J. Berdugo,²⁸ P. Berges,¹⁷ B. Bertucci,³⁶ B.L. Betev,⁵¹ S. Bhattacharya,¹¹ M. Biasini,¹⁹ A. Biland,⁵¹ G.M. Bilei,³⁶ J.J. Blaising,⁴ S.C. Blyth,³⁷ G.J. Bobbink,² R. Bock,¹ A. Böhm,¹ L. Boldizar,¹⁵ B. Borgia,³⁹ D. Bourilkov,⁵¹ M. Bourquin,²¹ S. Braccini,²¹ J.G. Branson,⁴² V. Brigljevic,⁵¹ I.C. Brock,³⁷ A. Buffini,¹⁸ A. Buijs,⁴⁷ J.D. Burger,¹⁷ W.J. Burger,²¹ J. Busenitz,⁴⁶ A. Button,³ X.D. Cai,¹⁷ M. Campanelli,⁵¹ M. Capell,¹⁷ G. Cara Romeo,¹⁰ G. Carlino,³¹ A.M. Cartacci,¹⁸ J. Casaus,²⁸ G. Castellini,¹⁸ F. Cavallari,³⁹ N. Cavallo,³¹ C. Cecchi,²¹ M. Cerrada,²⁸ F. Cesaroni,²⁵ M. Chamiz,²⁸ Y.H. Chang,⁵³ U.K. Chaturvedi,²⁰ S.V. Chekanov,³³ M. Chemarin,²⁷ A. Chen,⁵³ G. Chen,⁸ G.M. Chen,⁸ H.F. Chen,²² H.S. Chen,⁸ X. Chereau,⁴ G. Chiefari,³¹ C.Y. Chien,⁵ L. Cifarelli,⁴¹ F. Cindolo,¹⁰ C. Civinini,¹⁸ I.M. Clare,¹⁷ R. Clare,¹⁷ H.O. Cohn,³⁴ G. Coignet,⁴ A.P. Colijn,² N. Colino,²⁸ V. Commichau,¹ S. Costantini,⁹ F. Cotorobai,¹⁴ B. de la Cruz,²⁸ A. Csilling,¹⁵ T.S. Dai,¹⁷ R.D. Alessandro,¹⁸ R. de Asmundis,³¹ A. Degré,⁴ K. Deiters,⁴⁹ D. della Volpe,³¹ P. Denes,³⁸ F. DeNotaristefani,³⁹ D. DiBitonto,⁴⁶ M. Diemoz,³⁹ D. van Dierendonck,² F. Di Lodovico,⁵¹ C. Dionisi,³⁹ M. Dittmar,⁵¹ A. Dominguez,⁴² A. Doria,³¹ M.T. Dova,² D. Duchesneau,⁴ P. Duinker,² I. Duran,⁴³ S. Dutta,¹¹ S. Easo,³⁶ Yu. Efremenko,³⁴ H. El Mamouni,²⁷ A. Engler,³⁷ F.J. Eppling,¹⁷ F.C. Erné,² J.P. Ernenwein,²⁷ P. Extermann,²¹ M. Fabre,⁴⁹ R. Faccini,³⁹ S. Falciano,³⁹ A. Favara,¹⁸ J. Fay,²⁷ O. Fedin,⁴⁰ M. Felcini,⁵¹ B. Fenyi,⁴⁶ T. Ferguson,³⁷ F. Ferroni,³⁹ H. Fesefeldt,¹ E. Fiandrini,³⁶ J.H. Field,²¹ F. Filthaut,³⁷ P.H. Fisher,¹⁷ I. Fisk,⁴² G. Forconi,¹⁷ L. Fredj,²¹ K. Freudenreich,⁵¹ C. Furetta,²⁹ Yu. Galaktionov,^{30,17} S.N. Ganguli,¹¹ P. Garcia-Abia,⁵⁰ S.S. Gau,¹³ S. Gentile,³⁹ N. Gheordanescu,¹⁴ S. Giagu,³⁹ S. Goldfarb,²⁴ J. Goldstein,¹² Z.F. Gong,²² A. Gougas,⁵ G. Gratta,³⁵ M.W. Gruenewald,⁹ V.K. Gupta,³⁸ A. Gurtu,¹¹ L.J. Gutay,⁴⁸ B. Hartmann,¹ A. Hasan,³² D. Hatzifotiadou,¹⁰ T. Hebbeker,⁹ A. Hervé,¹⁹ W.C. van Hoek,³³ H. Hofer,⁵¹ S.J. Hong,⁴⁵ H. Hoorani,³⁷ S.R. Hou,⁵³ G. Hu,⁵ V. Innocenti,⁹ K. Jenkes,¹ B.N. Jin,⁸ L.W. Jones,³ P. de Jong,¹⁹ I. Josa-Mutuberria,²⁸ A. Kasser,²⁴ R.A. Khan,²⁰ D. Kamrad,⁵⁰ Yu. Kamyshkov,³⁴ J.S. Kapustinsky,²⁶ Y. Karyotakis,⁴ M. Kaur,^{20,◇} M.N. Kienzle-Focacci,²¹ D. Kim,³⁹ D.H. Kim,⁴⁵ J.K. Kim,⁴⁵ S.C. Kim,⁴⁵ Y.G. Kim,⁴⁵ W.W. Kinnison,²⁶ A. Kirkby,³⁵ D. Kirkby,³⁵ J. Kirkby,¹⁹ D. Kiss,¹⁵ W. Kittel,³³ A. Klimentov,^{17,30} A.C. König,³³ A. Kopp,⁵⁰ I. Korolko,³⁰ V. Koutsenko,^{17,30} R.W. Kraemer,³⁷ W. Krenz,¹ A. Kunin,^{17,30} P. Ladron de Guevara,²⁸ I. Laktineh,²⁷ G. Landi,¹⁸ C. Lapoint,¹⁷ K. Lassila-Perini,⁵¹ P. Laurikainen,²³ M. Lebeau,¹⁹ A. Lebedev,¹⁷ P. Lebrun,²⁷ P. Lecomte,⁵¹ P. Lecoq,¹⁹ P. Le Coultre,⁵¹ J.M. Le Goff,¹⁹ R. Leiste,⁵⁰ E. Leonardi,³⁹ P. Levchenko,⁴⁰ C. Li,²² C.H. Lin,⁵³ W.T. Lin,⁵³ F.L. Linde,^{2,19} L. Lista,³¹ Z.A. Liu,⁸ W. Lohmann,⁵⁰ E. Longo,³⁹ W. Lu,³⁵ Y.S. Lu,⁸ K. Lübelmeyer,¹ C. Luci,³⁹ D. Luckey,¹⁷ L. Luminari,³⁹ W. Lustermann,⁴⁹ W.G. Ma,²² M. Maity,¹¹ G. Majumder,¹¹ L. Malgeri,³⁹ A. Malinin,³⁰ C. Mañá,²⁸ D. Mangeol,³³ S. Mangla,¹¹ P. Marchesini,⁵¹ A. Marin,¹² J.P. Martin,²⁷ F. Marzano,³⁹ G.G.G. Massaro,² D. McNally,¹⁹ R.R. McNeil,⁷ S. Mele,³¹ L. Merola,³¹ M. Meschini,¹⁸ W.J. Metzger,³³ M. von der Mey,¹ Y. Mi,²⁴ A. Mihul,¹⁴ A.J.W. van Mil,³³ G. Mirabelli,³⁹ J. Mnich,¹⁹ P. Molnar,⁹ B. Monteleoni,¹⁸ R. Moore,³ S. Morganti,³⁹ T. Moulik,¹¹ R. Mount,³⁵ S. Müller,¹ F. Muheim,²¹ A.J.M. Muijs,² S. Nahn,¹⁷ M. Napolitano,³¹ F. Nessi-Tedaldi,⁵¹ H. Newman,³⁵ T. Niessen,¹ A. Nippe,¹ A. Nisati,³⁹ H. Nowak,⁵⁰ Y.D. Oh,⁴⁵ H. Opitez,¹ G. Organtini,³⁹ R. Ostonen,²³ C. Palomares,²⁸ D. Pandoulas,¹ S. Paoletti,³⁹ P. Paolucci,³¹ H.K. Park,³⁷ I.H. Park,⁴⁵ G. Pascale,³⁹ G. Passaleva,¹⁸ S. Patricelli,³¹ T. Paul,¹³ M. Pauluzzi,³⁶ C. Paus,¹ F. Pauss,⁵¹ D. Peach,¹⁹ Y.J. Pei,¹ S. Pensotti,²⁹ D. Perret-Gallix,⁴ B. Petersen,³³ S. Petrak,⁹ A. Pevsner,⁵ D. Piccolo,³¹ M. Pieri,¹⁸ J.C. Pinto,³⁷ P.A. Piroué,³⁸ E. Pistolesi,²⁹ V. Plyaskin,³⁰ M. Pohl,⁵¹ V. Pojidaev,^{30,18} H. Postema,¹⁷ N. Produit,²¹ D. Prokofiev,⁴⁰ G. Rahal-Callot,⁵¹ N. Raja,¹¹ P.G. Rancoita,²⁹ M. Rattaggi,²⁹ G. Raven,⁴² P. Razis,³² K. Read,³⁴ D. Ren,⁵¹ M. Rescigno,³⁹ S. Reucroft,¹³ T. van Rhee,⁴⁷ S. Riemann,⁵⁰ K. Riles,³ A. Robohm,⁵¹ J. Rodin,¹⁷ B.P. Roe,³ L. Romero,²⁸ S. Rosier-Lees,⁴ Ph. Rossetet,²⁴ W. van Rossum,⁴⁷ S. Roth,¹ J.A. Rubio,¹⁹ D. Ruschmeier,⁹ H. Rykaczewski,⁵¹ J. Salicio,¹⁹ E. Sanchez,²⁸ M.P. Sanders,³³ M.E. Sarakinos,²³ S. Sarkar,¹¹ M. Sassowsky,¹ C. Schäfer,¹ V. Schegelsky,⁴⁰ S. Schmidt-Kaerst,¹ D. Schmitz,¹ P. Schmitz,¹ N. Scholz,⁵¹ H. Schopper,⁵² D.J. Schotanus,³³ J. Schwenke,¹ G. Schwing,¹ C. Sciacca,³¹ D. Sciarino,²¹ L. Servoli,³⁶ S. Shevchenko,³⁵ N. Shivarov,⁴⁴ V. Shoutko,³⁰ J. Shukla,²⁶ E. Shumilov,³⁰ A. Shvorob,³⁵ T. Siedenbueg,¹ D. Son,⁴⁵ A. Sopczak,⁵⁰ B. Smith,¹⁷ P. Spillantini,¹⁸ M. Steuer,¹⁷ D.P. Stickland,³⁸ A. Stone,⁷ H. Stone,³⁸ B. Stoyanov,⁴⁴ A. Straessner,¹ K. Strauch,¹⁶ K. Sudhakar,¹¹ G. Sultanov,²⁰ L.Z. Sun,²² G.F. Susinno,²¹ H. Suter,⁵¹ J.D. Swain,²⁰ X.W. Tang,⁸ L. Tauscher,⁶ L. Taylor,¹³ Samuel C.C. Ting,¹⁷ S.M. Ting,¹⁷ M. Tonutti,¹ S.C. Tonwar,¹¹ J. Tóth,¹⁵ C. Tully,³⁸ H. Tuchscherer,⁴⁶ K.L. Tung,⁸ Y. Uchida,¹⁷ J. Ulbricht,⁵¹ U. Uwer,¹⁹ E. Valente,³⁹ R.T. Van de Walle,³³ G. Vesztegombi,¹⁵ I. Vetlitsky,³⁰ G. Viertel,⁵¹ M. Vivargent,⁴ R. Völkert,⁵⁰ H. Vogel,³⁷ H. Vogt,⁵⁰ I. Vorobiev,³⁰ A.A. Vorobyov,⁴⁰ A. Vorvolakos,³² M. Wadhwa,⁶ W. Wallraff,¹ J.C. Wang,¹⁷ X.L. Wang,²² Z.M. Wang,²² A. Weber,¹ F. Wittgenstein,¹⁹ S.X. Wu,²⁰ S. Wynnhoff,¹ J. Xu,¹² Z.Z. Xu,²² B.Z. Yang,²² C.G. Yang,⁸ X.Y. Yao,⁸ J.B. Ye,²² S.C. Yeh,⁵³ J.M. You,³⁷ An. Zalite,⁴⁰ Yu. Zalite,⁴⁰ P. Zemp,⁵¹ Y. Zeng,¹ Z. Zhang,⁸ Z.P. Zhang,²² B. Zhou,¹² G.Y. Zhu,⁸ R.Y. Zhu,³⁵ A. Zichichi,^{10,19,20} F. Ziegler,⁵⁰

- 1 I. Physikalisches Institut, RWTH, D-52056 Aachen, FRG[§]
III. Physikalisches Institut, RWTH, D-52056 Aachen, FRG[§]
 - 2 National Institute for High Energy Physics, NIKHEF, and University of Amsterdam, NL-1009 DB Amsterdam, The Netherlands
 - 3 University of Michigan, Ann Arbor, MI 48109, USA
 - 4 Laboratoire d'Annecy-le-Vieux de Physique des Particules, LAPP,IN2P3-CNRS, BP 110, F-74941 Annecy-le-Vieux CEDEX, France
 - 5 Johns Hopkins University, Baltimore, MD 21218, USA
 - 6 Institute of Physics, University of Basel, CH-4056 Basel, Switzerland
 - 7 Louisiana State University, Baton Rouge, LA 70803, USA
 - 8 Institute of High Energy Physics, IHEP, 100039 Beijing, China[△]
 - 9 Humboldt University, D-10099 Berlin, FRG[§]
 - 10 University of Bologna and INFN-Sezione di Bologna, I-40126 Bologna, Italy
 - 11 Tata Institute of Fundamental Research, Bombay 400 005, India
 - 12 Boston University, Boston, MA 02215, USA
 - 13 Northeastern University, Boston, MA 02115, USA
 - 14 Institute of Atomic Physics and University of Bucharest, R-76900 Bucharest, Romania
 - 15 Central Research Institute for Physics of the Hungarian Academy of Sciences, H-1525 Budapest 114, Hungary[‡]
 - 16 Harvard University, Cambridge, MA 02139, USA
 - 17 Massachusetts Institute of Technology, Cambridge, MA 02139, USA
 - 18 INFN Sezione di Firenze and University of Florence, I-50125 Florence, Italy
 - 19 European Laboratory for Particle Physics, CERN, CH-1211 Geneva 23, Switzerland
 - 20 World Laboratory, FBLJA Project, CH-1211 Geneva 23, Switzerland
 - 21 University of Geneva, CH-1211 Geneva 4, Switzerland
 - 22 Chinese University of Science and Technology, USTC, Hefei, Anhui 230 029, China[△]
 - 23 SEFT, Research Institute for High Energy Physics, P.O. Box 9, SF-00014 Helsinki, Finland
 - 24 University of Lausanne, CH-1015 Lausanne, Switzerland
 - 25 INFN-Sezione di Lecce and Università Degli Studi di Lecce, I-73100 Lecce, Italy
 - 26 Los Alamos National Laboratory, Los Alamos, NM 87544, USA
 - 27 Institut de Physique Nucléaire de Lyon, IN2P3-CNRS, Université Claude Bernard, F-69622 Villeurbanne, France
 - 28 Centro de Investigaciones Energeticas, Medioambientales y Tecnológicas, CIEMAT, E-28040 Madrid, Spain^b
 - 29 INFN-Sezione di Milano, I-20133 Milan, Italy
 - 30 Institute of Theoretical and Experimental Physics, ITEP, Moscow, Russia
 - 31 INFN-Sezione di Napoli and University of Naples, I-80125 Naples, Italy
 - 32 Department of Natural Sciences, University of Cyprus, Nicosia, Cyprus
 - 33 University of Nijmegen and NIKHEF, NL-6525 ED Nijmegen, The Netherlands
 - 34 Oak Ridge National Laboratory, Oak Ridge, TN 37831, USA
 - 35 California Institute of Technology, Pasadena, CA 91125, USA
 - 36 INFN-Sezione di Perugia and Università Degli Studi di Perugia, I-06100 Perugia, Italy
 - 37 Carnegie Mellon University, Pittsburgh, PA 15213, USA
 - 38 Princeton University, Princeton, NJ 08544, USA
 - 39 INFN-Sezione di Roma and University of Rome, "La Sapienza", I-00185 Rome, Italy
 - 40 Nuclear Physics Institute, St. Petersburg, Russia
 - 41 University and INFN, Salerno, I-84100 Salerno, Italy
 - 42 University of California, San Diego, CA 92093, USA
 - 43 Dept. de Física de Partículas Elementales, Univ. de Santiago, E-15706 Santiago de Compostela, Spain
 - 44 Bulgarian Academy of Sciences, Central Lab. of Mechatronics and Instrumentation, BU-1113 Sofia, Bulgaria
 - 45 Center for High Energy Physics, Korea Adv. Inst. of Sciences and Technology, 305-701 Taejeon, Republic of Korea
 - 46 University of Alabama, Tuscaloosa, AL 35486, USA
 - 47 Utrecht University and NIKHEF, NL-3584 CB Utrecht, The Netherlands
 - 48 Purdue University, West Lafayette, IN 47907, USA
 - 49 Paul Scherrer Institut, PSI, CH-5232 Villigen, Switzerland
 - 50 DESY-Institut für Hochenergiephysik, D-15738 Zeuthen, FRG
 - 51 Eidgenössische Technische Hochschule, ETH Zürich, CH-8093 Zürich, Switzerland
 - 52 University of Hamburg, D-22761 Hamburg, FRG
 - 53 High Energy Physics Group, Taiwan, China
- § Supported by the German Bundesministerium für Bildung, Wissenschaft, Forschung und Technologie
‡ Supported by the Hungarian OTKA fund under contract numbers T14459 and T24011.
^b Supported also by the Comisión Interministerial de Ciencia y Tecnología
‡ Also supported by CONICET and Universidad Nacional de La Plata, CC 67, 1900 La Plata, Argentina
△ Also supported by Panjab University, Chandigarh-160014, India
△ Supported by the National Natural Science Foundation of China.

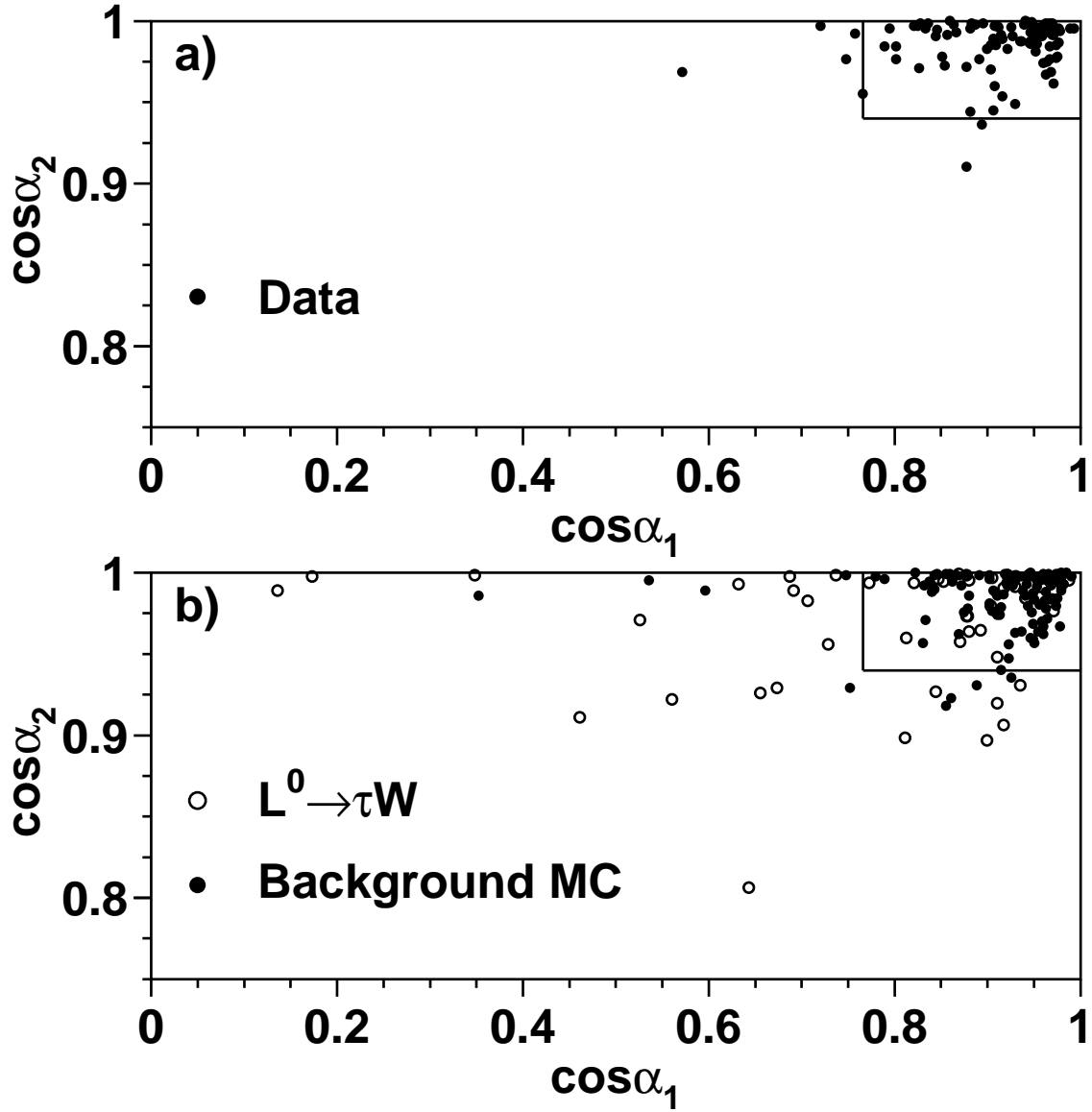


Figure 1: a) $\cos \alpha_1$ vs $\cos \alpha_2$, where α_1 is the angle between most isolated track and the track nearest to it and α_2 is the angle between the second most isolated track and the track nearest to it, for the data taken at $\sqrt{s} = 161$ GeV and 172 GeV. The lines represent the cut. b) $\cos \alpha_1$ versus $\cos \alpha_2$. The black circles represent the background Monte Carlo. The open circles are the predicted signal $e^+e^- \rightarrow L^0\bar{L}^0$, where L^0 is of the Dirac type with $m_{L^0} = 70$ GeV. The normalization for the signal Monte Carlo is scaled by a factor of 2 for better visibility. The lines represent the corresponding value of the applied cut.

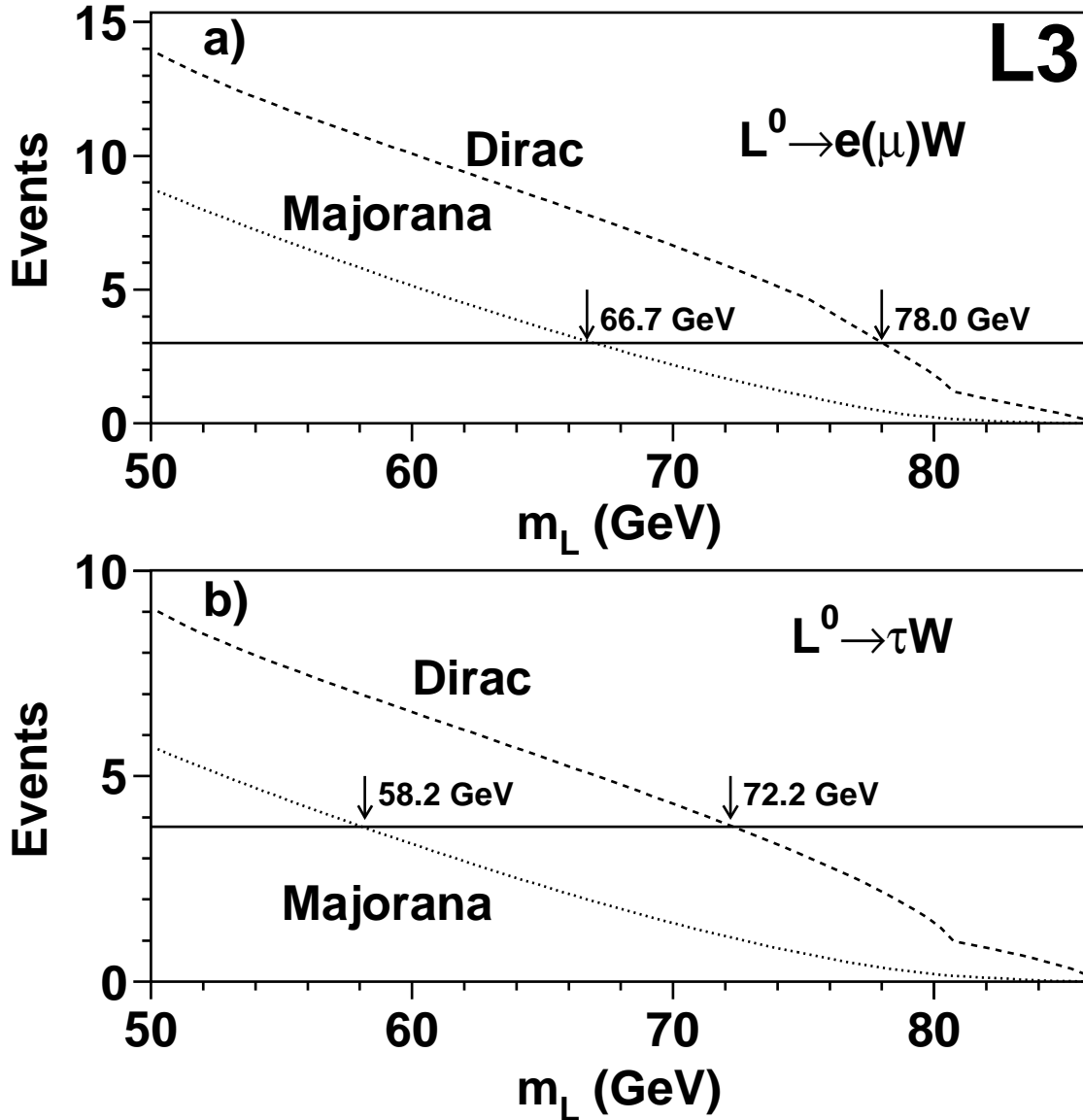


Figure 2: a) Expected number of events (in the 161 and 172 GeV data) as a function of neutral heavy lepton mass for decays into electrons or muons. The dashed and dotted curves represent the expectations for sequential Dirac and Majorana neutrinos, respectively. The line represents the 95% C.L. limit. The arrows indicate the 95% C.L. lower limit obtained for heavy neutral lepton mass. b) Expected number of events (in the 161 and 172 GeV data) as a function of the neutral heavy lepton mass for decays into taus.

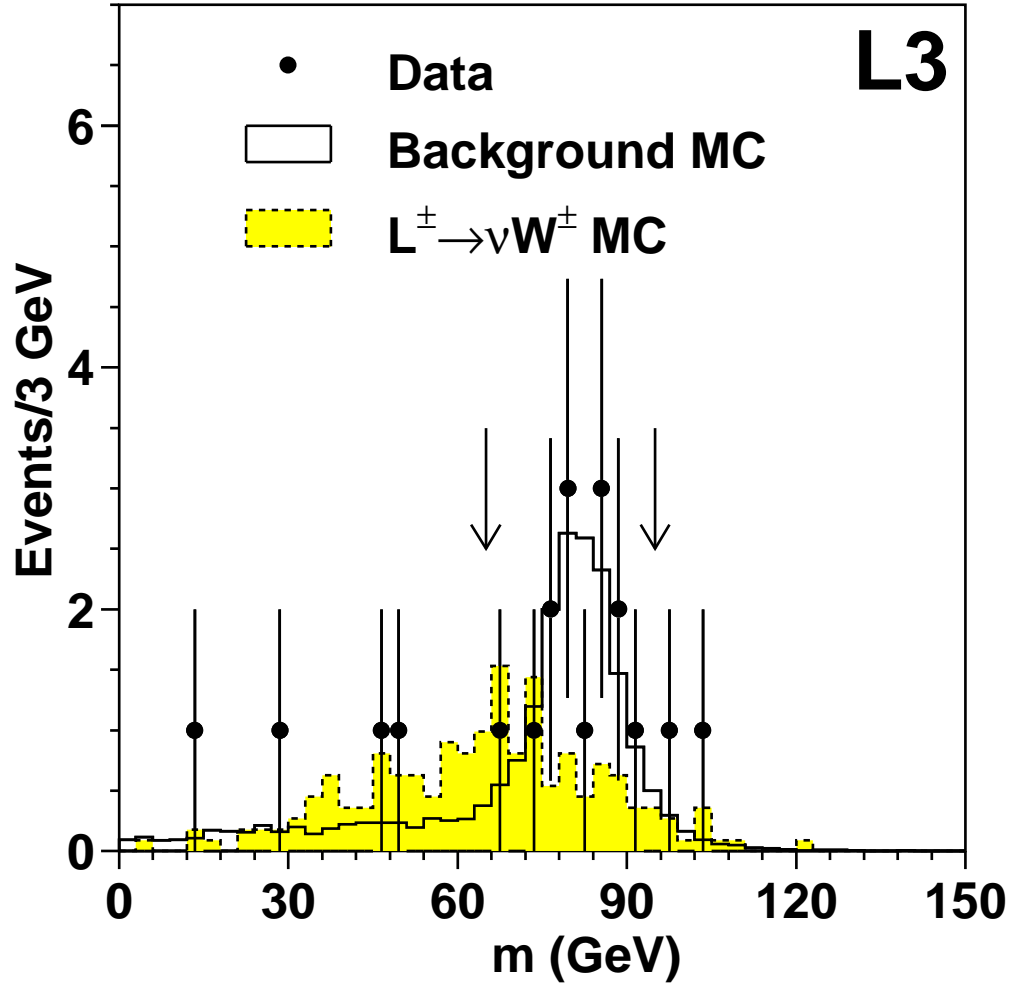


Figure 3: The invariant mass, m , of the isolated lepton and missing momentum. The dots are the data (taken at $\sqrt{s} = 161$ and 172 GeV), the solid histogram is the background Monte Carlo. The dashed histogram is a predicted signal $e^+e^- \rightarrow L^+L^-$ with $m_{L^\pm} = 75$ GeV. The normalization for the signal Monte Carlo is scaled by a factor of 2 for better visibility. The arrows indicate the corresponding value of the applied cut.

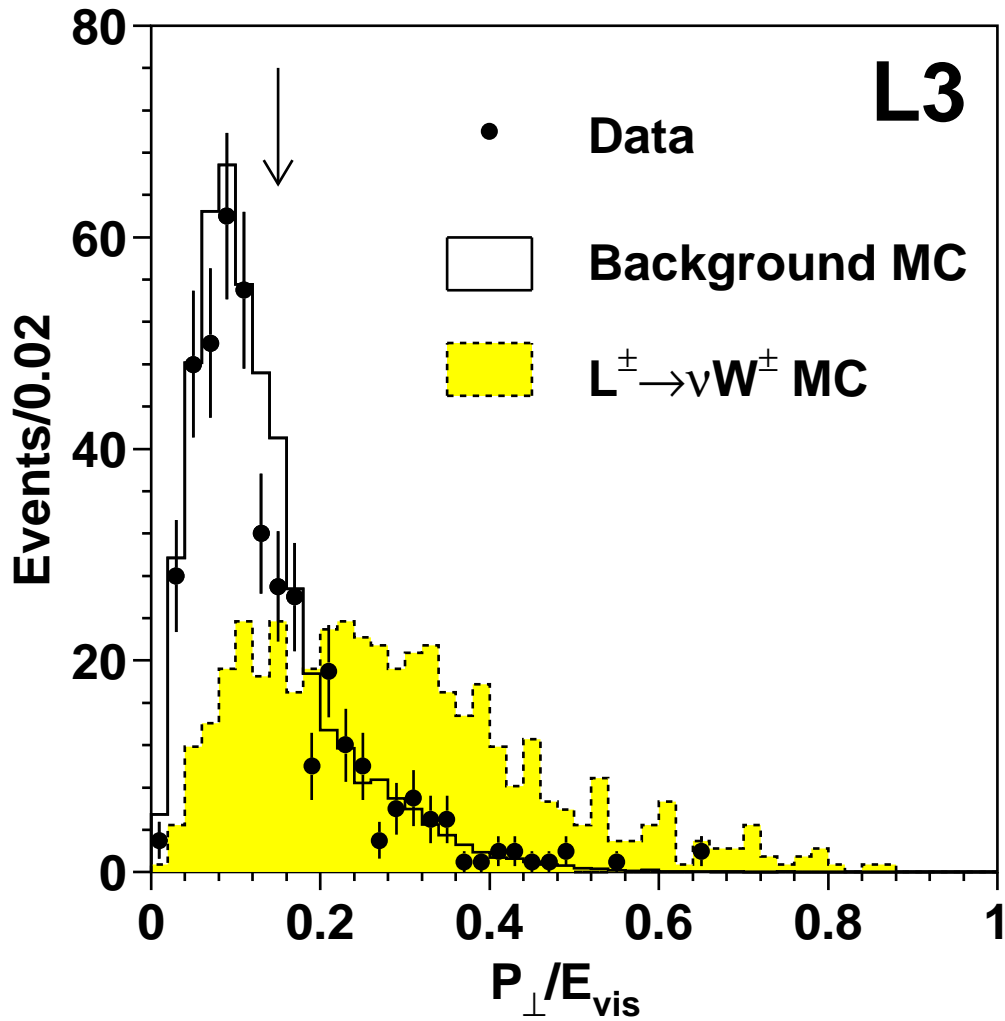


Figure 4: The distribution of the transverse momentum, P_{\perp} , normalised to the total visible energy, E_{vis} . The dots are the data (taken at $\sqrt{s} = 161$ GeV and 172 GeV), the solid histogram is the background Monte Carlo. The dashed histogram is a predicted signal $e^+e^- \rightarrow L^+L^-$ with $m_{L^{\pm}} = 75$ GeV. The normalization for the signal Monte Carlo is scaled by a factor of 10 for better visibility. The arrow indicates the corresponding value of the applied cut.

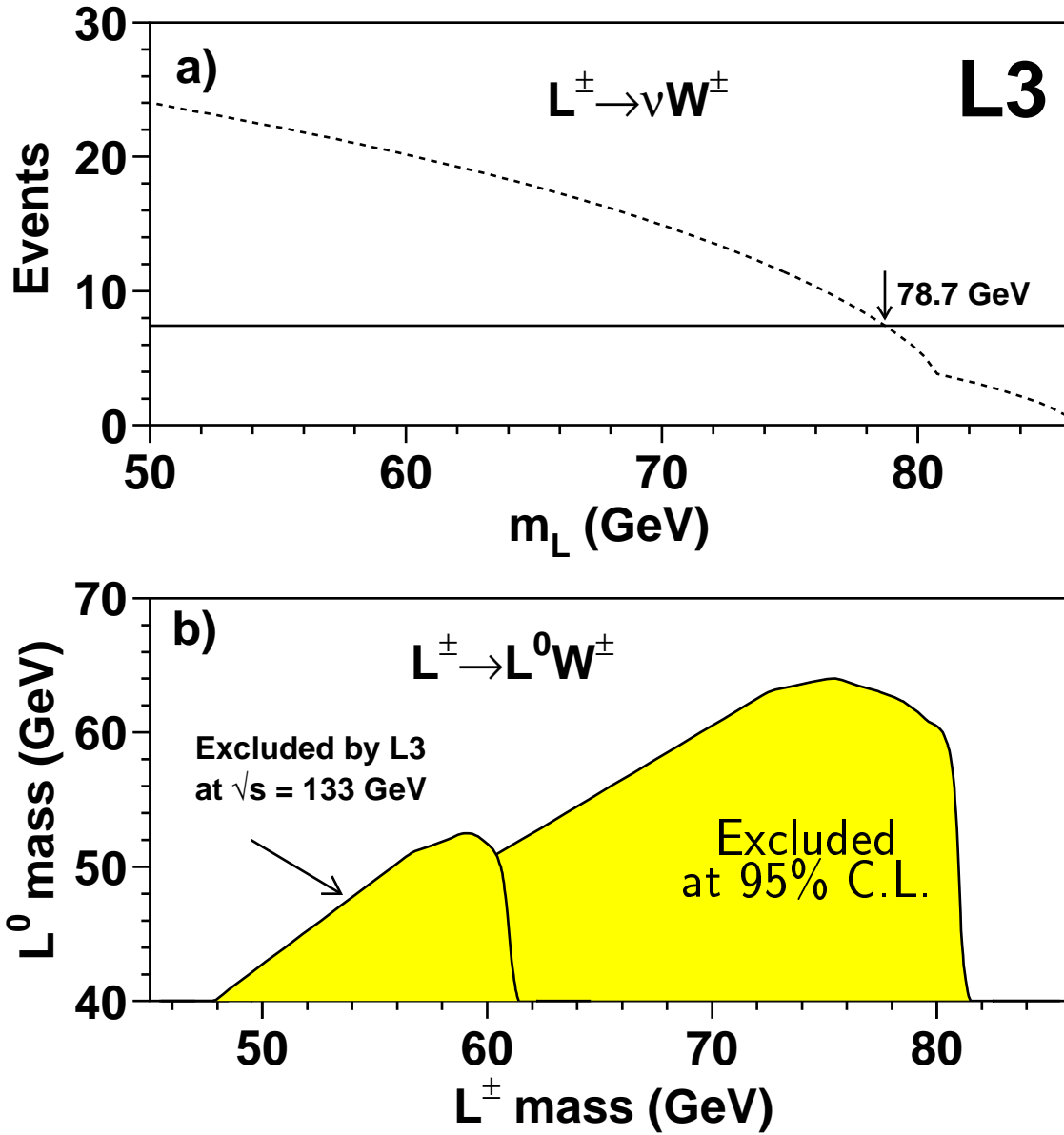


Figure 5: a) The dashed line represents the expected number of events (in the 161 and 172 GeV data) as a function of charged heavy lepton mass for decays into light neutrino. The arrow indicates the 95% C.L. lower limit obtained for heavy charged lepton mass. b) The 95% confidence level limits on the charged heavy lepton mass $m_{L^{\pm}}$ and the associated neutral heavy lepton mass m_{L^0} assuming L^0 is stable at $\sqrt{s} = 172$ GeV. Also shown is the limit from the previous L3 result at $\sqrt{s} = 133$ GeV.

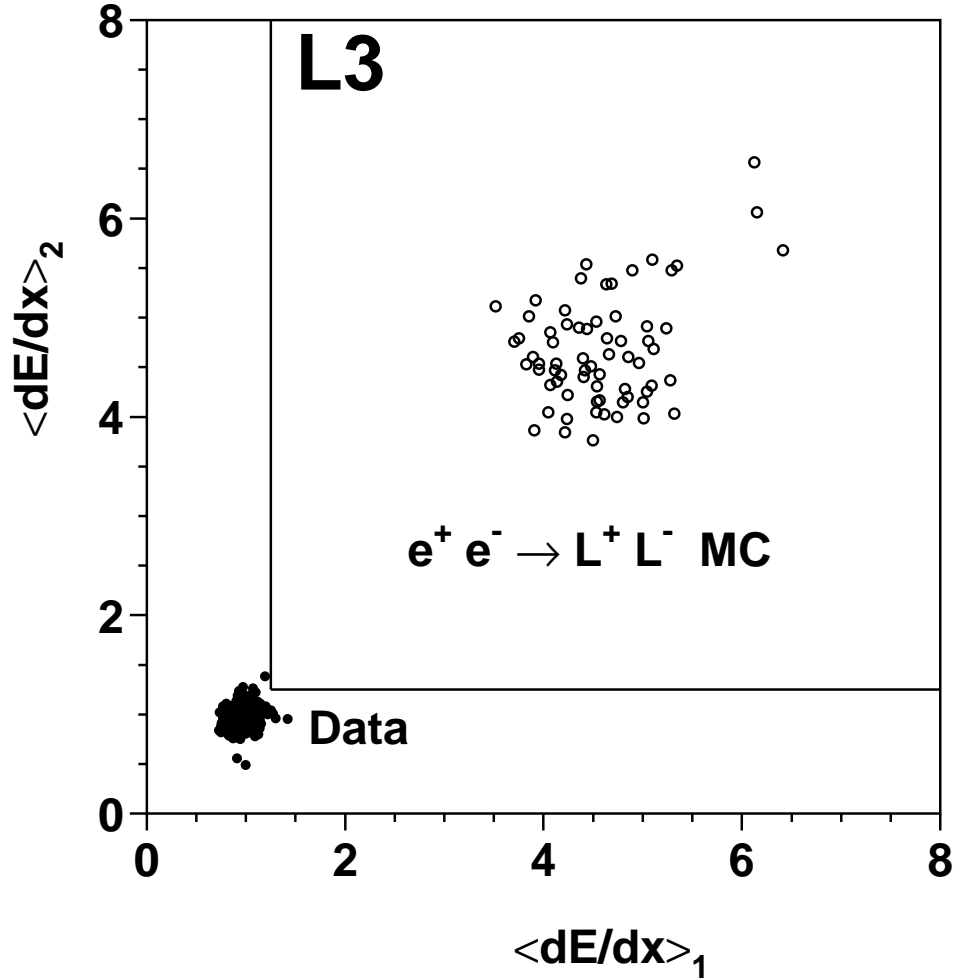


Figure 6: The normalized measured track energy loss of track 2 vs track 1 for the data (solid circles) taken at $\sqrt{s} = 172$ GeV and the expected signal (arbitrary normalization) for a mass 84 GeV stable heavy charged lepton (open circles). The lines represent the corresponding value of the applied cut.

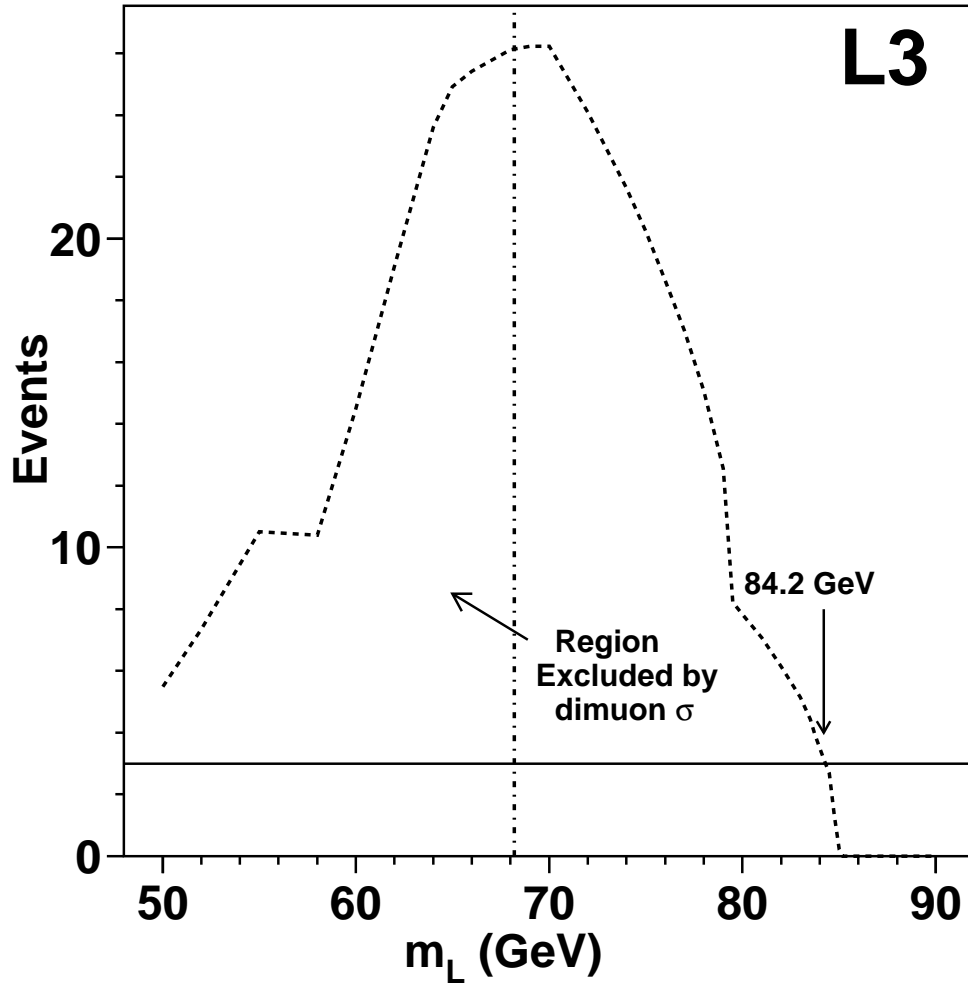


Figure 7: The dashed line represents the expected number of stable charged heavy lepton events in the L3 data at $\sqrt{s} = 133 - 172$ GeV as a function of mass. The solid line is the 95% C.L. limit in the data. The arrow indicates the 95% C.L. lower limit obtained for stable charged heavy lepton mass. Also indicated by the dot-dashed line is the region excluded by the dimuon cross section measurement.